nature COMMUNICATIONS

ARTICLE

Received 29 May 2013 | Accepted 2 Jul 2013 | Published 30 Jul 2013

DOI: 10.1038/ncomms3215 OPEN

A Munc13-like protein in *Arabidopsis* mediates H^+-ATPase translocation that is essential for stomatal responses

Mimi Hashimoto-Sugimoto[1], Takumi Higaki[2,3], Takashi Yaeno[4], Ayako Nagami[1], Mari Irie[1], Miho Fujimi[1], Megumi Miyamoto[1], Kae Akita[2], Juntaro Negi[1], Ken Shirasu[4], Seiichiro Hasezawa[2,3] & Koh Iba[1]

Plants control CO_2 uptake and water loss by modulating the aperture of stomata located in the epidermis. Stomatal opening is initiated by the activation of H^+-ATPases in the guard-cell plasma membrane. In contrast to regulation of H^+-ATPase activity, little is known about the translocation of the guard cell H^+-ATPase to the plasma membrane. Here we describe the isolation of an *Arabidopsis* gene, *PATROL1*, that controls the translocation of a major H^+-ATPase, AHA1, to the plasma membrane. *PATROL1* encodes a protein with a MUN domain, known to mediate synaptic priming in neuronal exocytosis in animals. Environmental stimuli change the localization of plasma membrane-associated PATROL1 to an intracellular compartment. Plasma membrane localization of AHA1 and stomatal opening require the association of PATROL1 with AHA1. Increased stomatal opening responses in plants overexpressing *PATROL1* enhance the CO_2 assimilation rate, promoting plant growth.

[1] Department of Biology, Faculty of Sciences, Kyushu University, Fukuoka 812-8581, Japan. [2] Department of Integrated Biosciences, Graduate School of Frontier Sciences, The University of Tokyo, Kashiwanoha Kashiwa, Chiba 277-8562, Japan. [3] Department of Advanced Measurement and Analysis, Japan Science and Technology Agency (JST), Chiyoda-ku, Tokyo 102-0076, Japan. [4] Plant Science Center, RIKEN, 1-7-22 Suehiro-cho, Tsurumi, Yokohama, Kanagawa 230-0045, Japan. Correspondence and requests for materials should be addressed to K.I. (email: koibascb@kyushu-u.org).

Stomatal pores, formed by pairs of guard cells, serve as major gateways for gas exchange between plants and their environments[1]. Opening of stomata is stimulated by low CO_2 concentrations and light, whereas stomatal closure occurs in response to high CO_2, darkness and shortage of water. Guard cells integrate these signals and appropriately adjust the stomatal pore apertures to optimize growth performance[2,3]. Stomatal opening is driven by an increase in guard-cell turgor when plasma membrane H^+-ATPases are activated through phosphorylation and induce membrane hyperpolarization facilitating K^+ entry into the guard cells[4,5]. Although the activity of plasma membrane H^+-ATPases is modulated by various physiological signals, there is little evidence that these factors alter the abundance of H^+-ATPase in the plasma membrane[6].

Here we describe a Munc13 ortholog named PATROL1 that in *Arabidopsis* controls the tethering of an H^+-ATPase, AHA1[7], to the plasma membrane, and demonstrate that PATROL1 function is essential for stomatal opening in response to low [CO_2] and light.

Results

The *patrol1* mutation impairs the stomatal opening response. Leaf temperature acts as a convenient indicator of transpiration and can help detect mutants with altered stomatal control[8,9]. *Arabidopsis ht* mutants were identified by higher leaf temperature than the wild type (WT) under low CO_2 conditions, as visualized by infrared imaging[9] (Fig. 1a). One of them, a recessive mutant originally referred to as *ht2* and here renamed *patrol1* (*proton ATPase translocation control 1*), was impaired in CO_2-dependent leaf temperature change (Fig. 1a) as well as in stomatal opening in response to low [CO_2] (Fig. 1b). The stomatal density of 3-week-old leaves was similar in WT and *patrol1* plants (136 ± 23.4 and 132 ± 23.6 stomata per mm^2 in WT and *patrol1*, respectively; means ± s.d.; $n = 20$ leaves). Thus, the high leaf temperature at low [CO_2] in *patrol1* could not be explained by stomatal density, but by a reduction of stomatal aperture.

***PATROL1* encodes a protein with MUN domain.** The *PATROL1* locus was mapped to a location between the Cereon single-nucleotide polymorphism marker, CER438918, and the original molecular marker moj9-47976, on chromosome 5 (Supplementary Fig. S1). Sequencing of this 47-kb region revealed that At5g06970 harboured a point mutation at nucleotide 2,156 that resulted in the exchange of Trp-318 for a stop codon (Fig. 1c,d). The 3.8-kb

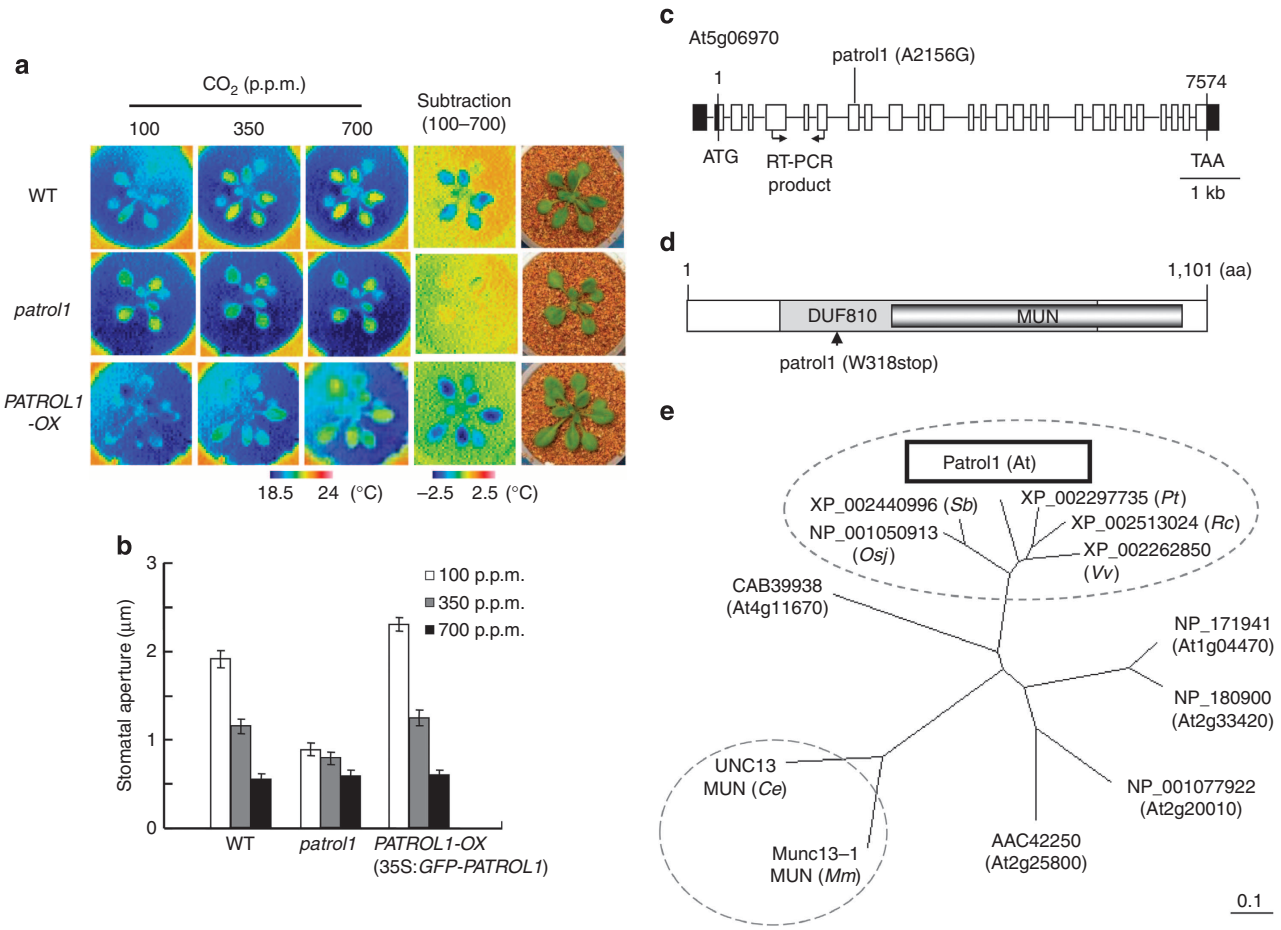

Figure 1 | The *Arabidopsis* Munc13-like protein PATROL1 is required for stomatal CO_2 response. (**a**) Three-week-old plants were subjected to the indicated [CO_2]. The subtractive images show changes in leaf temperature in response to the transfer from high to low [CO_2]. (**b**) CO_2 response of stomatal aperture in WT, *patrol1* mutants and 35S:*GFP-PATROL1*. Three-week-old plants were incubated at the indicated [CO_2]. Data are means ± s.e.m. ($n = 60$) of three independent experiments. (**c**) Structure of the *PATROL1* gene. *PATROL1* consists of 27 exons (white boxes); black boxes highlight the 5′ and 3′ untranslated regions, respectively. Arrows indicate regions used in RT-PCR (Supplementary Figs S2, S4). (**d**) *PATROL1* encodes a protein of unknown function with a MUN domain. DUF810 (IPR008528; 194–865 aa), MUN (428–1042 aa). (**e**) Phylogenetic relationships based on amino-acid sequence similarities between MUN domain-containing proteins and the MUN domains of Unc13/Munc13 proteins (UNC13-MUN (Ce: *C. elegans*), Munc13-1 MUN (Mm: *Mus musculus*)), as determined with CLUSTAL X. At, *Arabidopsis thaliana*; Rc, *Ricinus communis*; Vv, *Vitis vinifera*; Osj, *Oryza sativa subsp.japonica*; Sb, *Sorghum bicolor*; Pt, *Populus trichocarpa*.

PATROL1 cDNA fragment expressed under the control of the CaMV 35S promoter complemented the smaller mutant phenotype and restored the CO_2 response in stably transformed *patrol1* (35S:*PATROL1*) (Supplementary Fig. S2). This indicates that *PATROL1* is At5g06970, which encodes an uncharacterized protein with a Domain of Unknown Function 810 (DUF810) (Fig. 1c; InterPro; http://www.ebi.ac.uk/interpro/) of 1,101 amino acids. Plant proteins that have a MUN domain have been classified as DUF810 (Fig. 1d). Munc13 proteins are crucial components in neurotransmitter release in animals, controlling the priming of synaptic vesicles to the release-ready state[10,11]. Intracellular membrane fusion is generally dependent on the activities of SNARE complexes[12]. A large α-helical domain of mammalian Munc13-1, the MUN domain, dramatically accelerates the transition from the closed Syntaxin-1/Munc18-1 complex to the SNARE complex[13], and is sufficient for the activity of Munc13-1 in synaptic vesicle priming[14]. MUN domains are found in diverse proteins from animals, plants and fungi[15,16]. Munc13 proteins in animals have extensive conserved sequences and domains in addition to the MUN domain[16]. We compared the amino-acid sequences of the MUN domains of two representative Munc13 proteins. The animal MUN domains exhibit weak amino-acid identities with PATROL1 (Fig. 1e; 16% in Unc13-MUN (*C. elegans*) and 8% in Munc13-MUN (*Mus musculus*)). The sequence identities of *PATROL1* with five other *Arabidopsis* DUF810 members are not high (17–32%; Fig. 1e, Supplementary Fig. S3). On the other hand, higher plants including monocots and dicots have PATROL1 orthologues with highly conserved homologies distributed across the entire sequences (identities; 66–76%; Fig. 1e, Supplementary Fig. S3), suggesting an essential function. Computational biology and available three-dimensional (3D) structures indicate structural similarity between MUN domains of Munc13-related proteins including PATROL1 and other distantly related vesicle tethering factors such as the Exocyst, GARP, COG and Dsl1p complexes[16,17]. This suggests that PATROL1 may have a conserved function in intracellular membrane fusion.

Expression pattern of *PATROL1* in *Arabidopsis*. To examine the expression patterns of *PATROL1*, we used the PATROL1 promoter to drive expression of the GUS reporter (p*PATROL1*::*GUS*; Supplementary Fig. S4a–f), and RT-PCR analysis with gene-specific primers (Fig. 1c, Supplementary Fig. S4g,h). *PATROL1* was expressed in the whole plant, including guard cells (Supplementary Fig. S4). Global gene expression analysis of microarrays indicated that other DUF810 member genes in *Arabidopsis* were expressed mainly in floral organs (*At1g04470* and *At2g33420*) or in the whole plant (*At2g20010*, *At2g25800* and *At4g11670*), similar to *PATROL1*[18]. Two closely related genes (*At2g33420* and *At4g11670*) were expressed especially in mature pollen and pollen tubes, suggesting roles in pollen germination and tube growth[19]. Compared to other DUF810 member genes with pleiotropic expression, PATROL1 expression levels appeared relatively high[18], and the loss-of-function mutation in *PATROL1* impaired stomatal movement (Fig. 1b) and caused growth retardation (Supplementary Fig. S2), raising the possibility that *PATROL1* has a major function in stomatal response and plant growth.

Environmental conditions alter PATROL1 subcellular distribution. We generated transgenic plants expressing green fluorescent protein (GFP) fused to the N terminus of the full-length PATROL1 protein (GFP–PATROL1) to determine the intracellular localization of PATROL1. The GFP–PATROL1 rescued the *patrol1* mutant phenotype; the plants showed increased sensitivity to low $[CO_2]$ due to overexpression of the transgenes (Fig. 1a,b, Supplementary Fig. S2). The lipophilic dye FM4-64 is internalized in living cells through endocytosis and can be used to visualize the endocytic pathway from the plasma membrane to the tonoplast[20,21]. Two minutes after the transfer of GFP–PATROL1 transgenic plants into FM4-64 buffer, the fluorescent dye exhibited a punctate pattern typical of endosomes with little or no vacuolar staining in hypocotyl epidermal cells (Fig. 2a,b). The FM4-64 signal partially colocalized with the GFP–PATROL1 fluorescence signal (Fig. 2b), indicating that GFP–PATROL1 resides in an endosomal compartment. This finding paralleled results from mouse brain cells, where signals from Munc13-1-EYFP and FM4-64 also colocalized[22]. When incubated in the dark for 72 h, numerous small structures showing GFP–PATROL1 fluorescence were observed in the guard cells of leaves in transgenic plants (Fig. 2c,d; dark); their number decreased after 30 min in the light (Fig. 2c,d; light for 30 min). The structures were rare in the guard cells of well-watered and irradiated plants, when most of the GFP–PATROL1 fluorescence was detected in close proximity to the plasma membrane (Fig. 2e,f; detached for 0 min). Within 30 min after detachment of the leaves, small fluorescent structures were observed inside the cell (Fig. 2e,f; detached for 30 min). These findings suggest that GFP–PATROL1 moved reversibly between the cytoplasm and the plasma membrane depending on environmental conditions.

Mutation of *PATROL1* causes altered localization of AHA1. If PATROL1 has a role in intracellular membrane traffic, it might control the localization of ion transporters that are crucial to stomatal opening (for example, plasma membrane H^+-ATPases). Stomatal opening is initiated by hyperpolarization of the guard-cell plasma membrane caused by H^+-ATPase-dependent proton efflux[5]. Membrane hyperpolarization activates inward-rectifying potassium channels and induces solute influx followed by water uptake into guard cells[4]. *Arabidopsis* H^+-ATPase 1 (AHA1) is highly expressed in guard cells and its activation induces stomatal opening[7,23]. We generated transgenic plants containing a *GFP–AHA1* fusion gene in the WT (AHA1/WT) and *patrol1* (AHA1/*patrol1*) background. In WT guard cells, GFP–AHA1 was localized mainly at the plasma membrane (Fig. 3a) as expected[24]. The internalization rate calculated from the number of guard cells that exhibited small fluorescent structures in their cytosol was 80% in AHA1/*patrol1* transgenic plants (Fig. 3a,b). This rate was significantly higher than that of AHA1/WT transgenic plants (8%; Fig. 3a,b), indicating that PATROL1 affects AHA1 localization to the plasma membrane. The slow anion channel SLAC1 contributes to anion efflux from guard cells and causes membrane depolarization, resulting in stomatal closure[25,26]. We compared the distribution of SLAC1–GFP fluorescence in transgenic WT and *patrol1* plants. Little internalization was observed in the guard cells of SLAC1–GFP transgenic plants even in the *patrol1* background (SLAC1/WT, 1%; SLAC1/*patrol1*, 3%; Fig. 3a,b). We examined another transporter, aquaporin PIP1a, which is localized in the plasma membrane of guard cells[27]. GFP–PIP2a has been used as a plasma membrane protein marker[28], and we also detected GFP fluorescence in the plasma membrane (GFP–PIP2a/WT, Fig. 3a,b). In the *patrol1* background, the internalization rate of GFP–PIP2a was slightly increased but remained low (PIP2a/WT, 0%; PIP2a/*patrol1*, 8.6%; Fig. 3a,b). These results indicated that PATROL1 is target-selective, as it is required for the direction of AHA1 to the plasma membrane, but less so for SLAC1 or PIP2a. We also examined the localization of the inward-rectifying potassium channel, KAT1, in *patrol1* mutants. This voltage-gated channel is activated by hyperpolarization, and mediates the influx

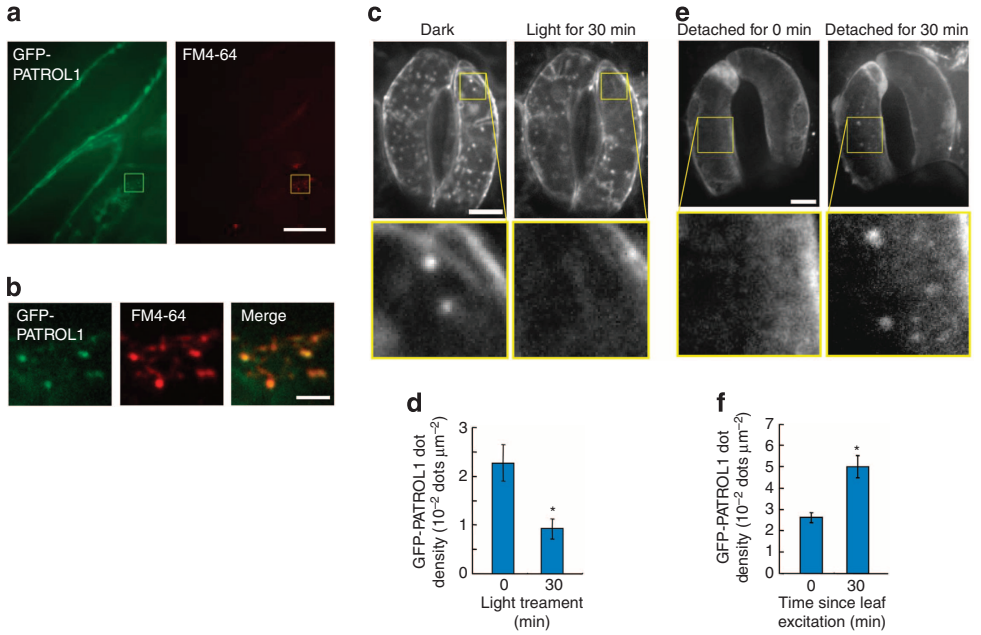

Figure 2 | Endosome-localized PATROL1 changes its distribution in response to environmental conditions. (**a**,**b**) Endosomal localization of GFP–PATROL1. Images of GFP–PATROL1 (green) and FM4-64 (red) in hypocotyl epidermal cells. The yellow square in (**a**) shows the part of the image that is enlarged in (**b**). Scale bars indicate 20 µm in (**a**) and 2 µm in (**b**). (**c**,**d**) GFP–PATROL1 localization changes in response to irradiation. Data are means ± s.e.m. of four to seven independent guard cells. (**e**,**f**) GFP–PATROL1 localization changes in response to drought stress after leaf detachment. Data are means ± s.e.m. of three independent guard cells. Asterisks indicate statistical significance (*$P<0.05$) as determined by Welch's *t*-test. Scale bars = 5 µm in (**c**) and (**e**).

of potassium into guard cells[29]. We could only slightly detect punctate structures of KAT1–GFP fluorescence in *patrol1* mutants, indicating that PATROL1 does not affect KAT1 localization to the plasma membrane (KAT1/WT, 0.6%; KAT1/*patrol1*, 1.1%; Supplementary Fig. S5). To our knowledge, the KAT1–GFPfluorescence in WT chloroplast envelopes that we detected has never been discussed before, but some figures in a previous report[30] showed similar localization. Among the four GFP-tagged plasma membrane-localized proteins in our transgenic plants, the fluorescence intensity of GFP–AHA1 was the strongest. As overexpressed membrane-targeted GFP fusion proteins have a propensity to form organelle aggregates as a consequence of oligomerization[31], we examined whether the increased internalization rate of the GFP–AHA1 in the *patrol1* mutant was caused by GFP. The monomeric red fluorescent protein (mRFP) contains 33 mutations compared to DsRed and was designed as a non-oligomerizing, true monomer[32]. The RFP-tagged AHA1 in the *patrol1* mutant appeared as numerous punctate structures in the cytosol (Fig. 3c), while it exhibited an extremely low fluorescence intensity in the plasma membrane (Fig. 3d,e), indicating apparent mislocalization of AHA1. We further attempted to identify plasma membrane H^+-ATPases in the epidermis of rosette leaves using anti-H^+-ATPase antibodies (anti-AHA) (Supplementary Fig. S6). The mean value of the fluorescent intensity from immunohistochemical staining in *patrol1* was slightly but not statistically significantly lower than in the WT (266.1 in arbitrary unit in WT, 288.3 in arbitrary unit in *patrol1*, respectively; $P=0.24$, Supplementary Fig. S6). One reason why no clear difference could be observed is that this method has the potential to detect not only plasma membrane AHA but also AHA in endosomes. Actually, intracellular localization of the H^+-ATPase has been found by this method, probably due to an artifact caused by the fixation for immunohistochemical detection[33]. It also seemed extremely difficult to distinguish endosomal AHA from plasma membrane AHA in guard cell protoplast proteins and to quantify their amounts. In order to estimate the amount of functional H^+-ATPases in the plasma membrane of guard cells, we investigated stomatal apertures when H^+-ATPases were compulsorily activated. The fungal phytotoxin fusicoccin (FC) induces irreversible stomatal opening by the continuous activation of the plasma membrane H^+-ATPases due to inhibition of their dephosphorylation in guard cells[5,34]. Though *Arabidopsis* has at least 11 plasma membrane H^+-ATPases and all of which are expressed in guard cells[23], the stomatal response to FC was severely impaired in *patrol1* (Fig. 3f; <0.5, unpaired two-tailed *t*-test), suggesting that the recruitment of functional H^+-ATPases to the plasma membrane was disturbed by the mutation. Thus, PATROL1 may have a crucial role in the recruitments of not only AHA1 but also of the other H^+-ATPases. 35S:*PATROL1* and 35S:*GFP–PATROL1* transgenic plants showed rather strong FC responses indicating increased AHA level in the plasma membrane (Fig. 3f). To obtain further insights into the relationship between PATROL1 and AHA1, we generated transgenic plants co-expressing GFP–PATROL1 and RFP–AHA1. In hypotonic conditions, which lead to stomatal opening, RFP–AHA1 was located in the plasma membrane, while GFP–PATROL1 seemed to line the membrane (Fig. 4a). In hypertonic conditions, which induce stomatal closure, RFP–AHA1 partially remained in the plasma membrane and GFP–PATROL1 seemed to support it. They resided on the plasma membrane–cell wall connection spots, that is, the tips of Hechtian strands in a plasmolyzed guard cells (Fig. 4b, arrows). These relationships suggest that PATROL1 contributes to H^+-ATPase localization to the plasma membrane.

Stomatal opening and CO_2 uptake in *PATROL1-OX* plants. To characterize the function of *PATROL1*, we compared the phenotypes of the *patrol1* mutant and the *PATROL1*-overexpressing

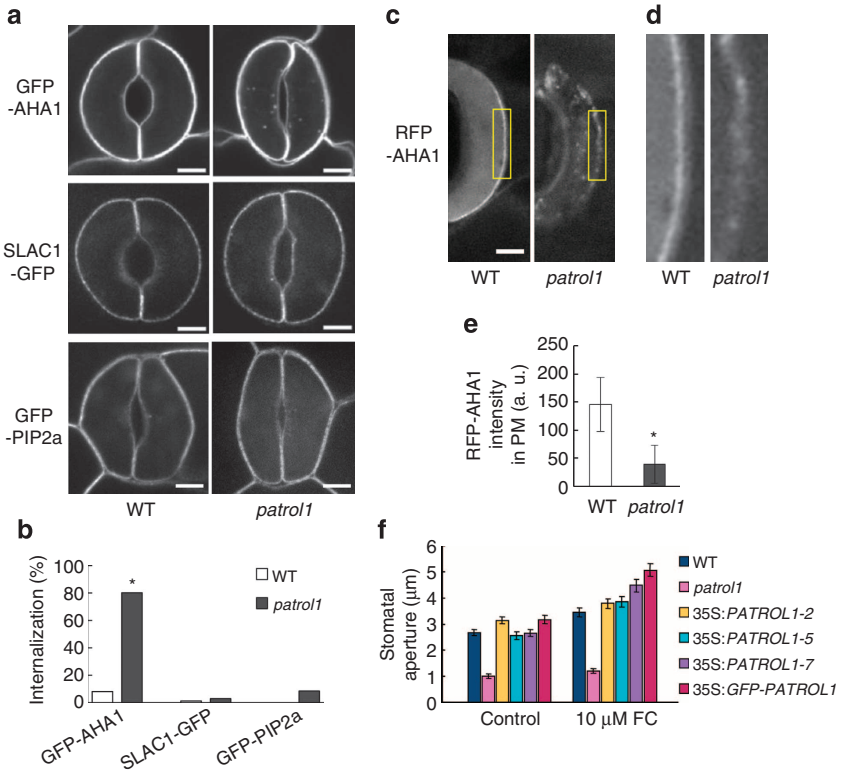

Figure 3 | *patrol1* mutation perturbs the plasma membrane localization of AHA1. (**a**) Optical sections showing the GFP–AHA1, SLAC1–GFP and GFP–PIP2a signals in guard cells in transgenic WT and *patrol1* plants. The *patrol1* mutation caused mislocalization of GFP–AHA1, which showed as internalized dots. Scale bars = 5 μm. (**b**) Percentages of guard cells of GFP–AHA1, SLAC1–GFP and GFP–PIP2a plants with 0.05 dots per μm^2 or denser. Around 197–269 guard cells were examined. Maximum intensity projection images reconstructed from serial optical sections, captured from the guard cell surface to the mid-plane with 1-μm intervals, were evalated. Asterisk indicates statistical significance ($P<0.001$, Ryan's test.) (**c**) Optical sections of RFP–AHA1-expressing guard cells in transgenic WT and *patrol1* plants. Scale bar = 5 μm. (**d**) Enlarged sectors of images on the (**c**). (**e**) Intensities of RFP–AHA1 fluorescence in the plasma membrane. Resions of the plasma membrane were determined with cytosolic fluorescein diacetate staining. Data are mean values ± s.d. of 10 independent guard cells. Asterisk indicates statistical significance (*$P<0.0001$, unpaired two-tailed *t*-test) (**f**) Effect of FC on stomatal opening. Data are means ± s.e.m. of 60 apertures measured in three independent experiments.

line (Supplementary Fig. S2c). 35S:*GFP–PATROL1* (hereafter *PATROL1-OX*) exhibited functional complementation of *patrol1*, including restored sensitivity to FC (Fig. 3f) and low [CO_2] (Fig. 1a, Supplementary Fig. S2b). *PATROL1-OX* exhibited lower leaf temperature under low [CO_2] than the WT due to enhanced stomatal opening (Fig. 1a,b). The rises in stomatal conductance in response to low [CO_2] and light were more rapid and reached higher maximum values (sometimes followed by oscillations) in *PATROL1-OX* than in the WT, whereas those in *patrol1* were slow and ceased at low values (Fig. 5a,c). Enhanced stomatal opening responses in *PATROL1-OX* plants may contribute to higher CO_2 assimilation rates even under low [CO_2] (Fig. 5a–d). Under normal or increased [CO_2], *PATROL1-OX* plants exhibited similar but slightly higher stomatal conductance compared to the WT. However, this small difference may be sufficient to elevate the CO_2 assimilation rate (Fig. 5a,b). We examined the response to desiccation stress in *PATROL1-OX* plants. The rate of transpirational water loss, evaluated as the fresh weight decrease of the excised *PATROL1-OX* leaves, resembled that of the WT. This was unlike the response found in the ABA-deficient mutant *aba2-1*[35] that showed excessive water loss owing to constitutive stomatal opening (Fig. 5e). These results suggested that *PATROL1-OX* plants control the stomatal aperture efficiently; they could open their stomata wider than the WT to maintain higher CO_2 assimilation rates, and close them to prevent extra water loss depending on the environmental conditions (Fig. 5).

***PATROL1-OX* plants exhibit enhanced growth**. When grown under continuous light for 20 days, *patrol1* plants were significantly smaller than the WT (Fig. 6a,b, analysis of variance (ANOVA), $P = 1.7 \times 10^{-11}$, *post hoc* Tukey tests, $P = 2.4 \times 10^{-7}$), whereas *PATROL1-OX* plants were bigger (in terms of above-ground fresh weight; Fig. 6a,b, *post hoc* Tukey tests, $P = 0.0496$). Thus, plant size correlated with CO_2 assimilation rate under standard [CO_2] (350 p.p.m.; Fig. 5b,d). Likewise, when grown for 7 weeks under short-day conditions (8 h light, 16 h dark), *PATROL1-OX* plants were 32% bigger than the WT (Fig. 6d,e, ANOVA, $P = 1.17 \times 10^{-4}$, *post hoc* Tukey tests, $P = 1.2 \times 10^{-3}$), although *patrol1* rosettes reached the size of WT ones (Fig. 6d,e, *post hoc* Tukey tests, $P = 0.75$). Compared to the WT, shorter and longer inflorescence stems were observed in *patrol1* and *PATROL1-OX*, respectively, when grown under continuous light for a month (Fig. 6c). Similar results were obtained when plants were grown first under short-day conditions for 7 weeks and then shifted to long-days to induce flowering for 2 more weeks (Fig. 6f). Taken together, PATROL1 affects not only stomatal movement but also leaf growth and stem elongation.

Discussion

In animals, Munc13 proteins are important for synaptic exocytosis and for cytotoxic granule exocytosis in NK cells[36]. Animal Munc13 proteins possess several conserved domains including Ca^{2+}-binding sites and/or domains required for

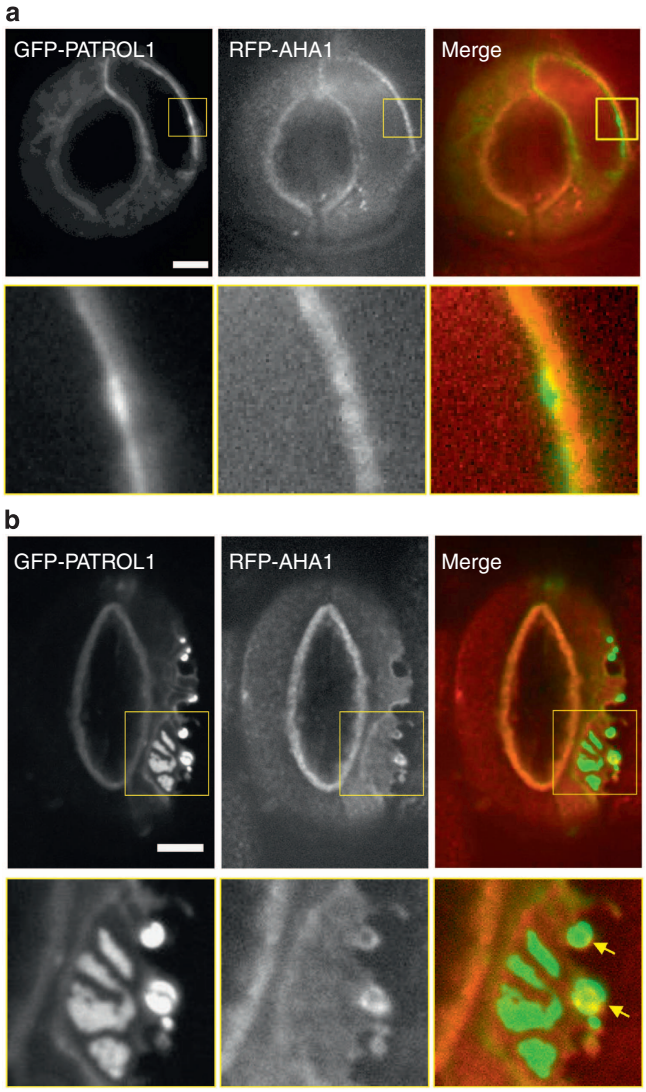

Figure 4 | PATROL1 lines with plasma membrane-localized AHA1. Subcellular localizations of GFP–PATROL1 and RFP–AHA1 in co-expressing transgenic plants under hypo-osmotic (**a**; 120 mOsM) and hyper-osmotic (**b**; 530 mOsM) conditions. (**a**,**b**) Enlarged images of the region enclosed in the yellow square are shown directly below. Scale bars = 5 μm. (**a**) RFP–AHA1 in the plasma membrane was lined by PATROL1 under hypotonic condition. (**b**) RFP–AHA1 and GFP–PATROL1 remain at the tips of Hechtian strands in plasmolyzed guard cells. The remaining positions are indicated by arrows.

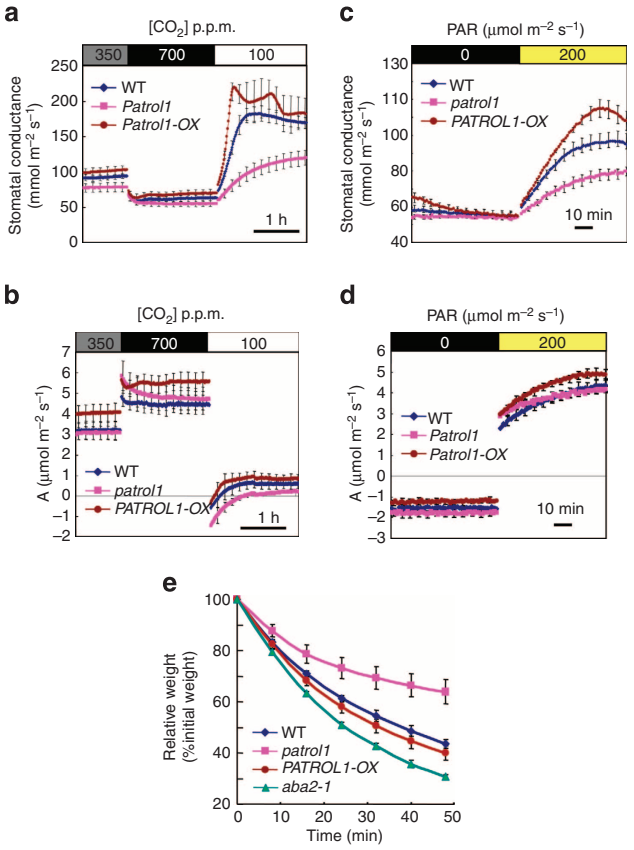

Figure 5 | *PATROL1*-overexpressing plants enhance stomatal conductance and CO_2 assimilation without dessication. (**a**–**d**) Stomatal conductance and CO_2 assimilation rate in response to [CO_2] changes (**a**,**b**), and to light (**c**,**d**). [CO_2] and light intensity were changed as indicated. Data represent means ± s.e.m. (**a**,**b**, $n = 4$; **c**,**d**, $n = 5$) from 3–4-week-old plants. (**e**) Kinetics of water loss from the aerial parts of WT, *patrol1*, *PATROL1-OX* and *aba2-1* plants. Water loss is expressed as the percentage of initial fresh weight. Values are means ± s.d. ($n = 4$). *patrol1* plants show reduced water loss, while *PATROL1-OX* plants exhibit normal values. As a wilty mutant control, *aba2-1* was used.

homodimerization[36]. Metazoan and fungal MUN domain-containing proteins carry C2 domains suggesting roles in regulating Ca^{2+}-dependent exocytosis. In plants, MUN domain-containing proteins are relatively smaller and have no known domains other than MUN[16]. This might suggest that Munc13-like proteins in plants do not need Ca^{2+} binding or need other Ca^{2+} binding components for its activation. In plants, the functions of Munc13-like genes are generally unknown. In this study, we showed that one of the *Arabidopsis* Munc13-like genes, *PATROL1*, has a role in stomatal responses and growth by regulation of the plasma membrane H^+-ATPase. We found that PATROL1 orthologues in higher plants have high identity and similarity to AtPATROL1 including a part adjacent to the MUN domain (Supplementary Fig. S4). These parts may be required for functions unique to plants that need to integrate signals received from the environment including light, CO_2 and humidity. H^+-ATPases are known to contribute to stomatal opening, cell elongation, and the growth of root hairs and pollen tubes[5]. Some of the DUF810 family genes have been reported to be expressed in pollen[18], suggesting functions in pollen germination and tube growth[19]. Thus, these genes may also have a role in H^+-ATPase tethering on the plasma membrane in pollen tubes.

Endosomes traffic biosynthetic cargo and recycle endocytosed plasma membrane components back to the plasma membrane. We showed that PATROL1 resides in the endosome and moves to and from the plasma membrane in response to environmental stimuli (Fig. 2). Under light and well-watered conditions that induce stomatal opening, PATROL1 mainly was found close to the plasma membrane, whereas under dark or dry conditions that induce stomatal closure, PATROL1 moved away from the plasma membrane (Fig. 2). The AHA1 in the plasma membrane was always associated with PATROL1 on the inside of the plasma membrane (Fig. 4). These facts are consistent with the function of PATROL1 in tethering H^+-ATPases to the plasma membrane. Stomatal movements by guard-cell swelling or shrinking require changes of guard-cell surface area through exocytotic addition or endocytotic retrieval of membrane[37,38]. When stomata open, intracellular vesicles incorporate with the plasma membrane

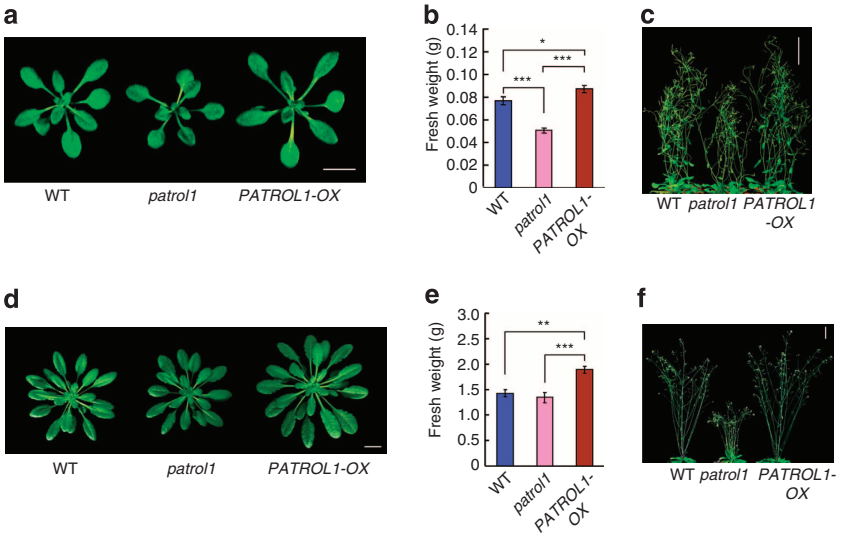

Figure 6 | Leaf growth is promoted in *PATROL1*-overexpressing plants. (**a**–**c**) Plants grown under continuous light for 20 (**a**,**b**), and 34 days (**c**). (**d**–**f**) Plants grown under short-day conditions for 7 weeks (**d**,**e**) and further grown under continuous light for 2 weeks (**f**). (**b**,**e**) Fresh weight of aerial parts of the plants. Data are means ± s.e.m.; $n = 21$ (**b**) or $n = 10$ (**e**). Statistical significance was analysed by ANOVA tests (20 days $P = 1.7 \times 10^{-11}$; 7 weeks $P = 1.17 \times 10^{-4}$) followed by a *post hoc* Tukey test. Asterisks (*$P < 0.05$, **$P < 0.005$, ***$P < 0.001$) indicate statistical significance. Scale bars = 1 cm in (**a**) and (**d**), and 5 cm in (**c**) and (**f**).

and PATROL1 may be carried with them to tether H^+-ATPases into the plasma membrane. In plasma membrane H^+-ATPases, changes in transcriptional levels are often uncoupled from changes in protein activities and/or proton fluxes[6]. It is therefore likely that post-translational modifications determine H^+-ATPase activity. Phosphorylation of H^+-ATPases and the phosphorylation-dependent binding of 14-3-3 protein are well-studied examples of post-translational regulation[5]. Modifications of the H^+-ATPase concentration in the plasma membrane are an alternative means to control total activity, but few studies addressed this alternative regulatory pathway[6]. A nonsense mutation just before the MUN domain of PATROL1 (Fig. 1d) resulted in irregular pattern of AHA1 distribution (Fig. 3a–e). In addition, *patrol1* showed defects in FC-, low CO_2- and light-induced stomatal opening (Figs 3f,5a,c), which supports the notion that the translocation of H^+-ATPases to the plasma membrane is an essential process in stomatal function that is controlled by PATROL1.

Furthermore, we showed that higher CO_2 assimilation rates increase biomass production in *PATROL1*-overexpressing plants. An *Arabidopsis* SNARE protein, syntaxin SYP121, functions in the anchoring of K^+ channels to the plasma membrane through direct physical interaction[39]. The *syp121* mutant exhibits delayed stomatal opening and develops similar or smaller rosettes than the WT depending on environmental conditions[30], similar to *patrol1*. This seems to indicate that membrane traffic generally controls stomatal movement, and consequently, plant growth. Dominant-negative Sp2 fragments of SYP121 from *Arabidopsis* and maize do not affect the plasma membrane delivery of the H^+-ATPase PMA2[40]. Taken together, SNARE proteins select their target plasma membrane proteins directly. PATROL1 may select its target H^+-ATPases indirectly by interacting with specific SNARE proteins and control the total amount of the plasma membrane H^+-ATPases. In this study, the *patrol1* mutation severely impaired the localization of AHA1 but did not affect that of KAT1, indicating that the target SNARE protein PATROL1 associates with may be different from SYP121. Auxin, a plant growth hormone, inhibits endocytosis of plasma membrane proteins and increases the density of H^+-ATPases in the PM[41]. H^+-ATPase acidifies the apoplast and loosens the cell wall leading to cell expansion[42]. As *PATROL1* is expressed in the entire plant (Supplementary Fig. S4), an increased accumulation of H^+-ATPases in the plasma membrane of various cell types may contribute to the enhanced growth in *PATROL1-OX* (Fig. 6). The constitutive activation of H^+-ATPases induces stomatal opening, but plants with continuously opened stomata often show comparatively small size and increased susceptibility to drought stress[7,43]. *PATROL1-OX* exhibited normal resistance against water loss (Fig. 5e). The ability to prevent water loss may contribute to the increased biomass production in *PATROL1-OX*. Overexpression of H^+-ATPase genes does not always enhance growth because of the downregulation of H^+-ATPase activity induced by the overexpression of its gene[43,44]. The nature of this feedback mechanism has not been elucidated yet. Similarly, overexpression of *AHA1* did not induce biomass increase and rather decreased biomass production in this study (Supplementary Fig. S7). On the contrary, overexpression of *PATROL1* increased biomass even in an *AHA1* overexpression background (Supplementary Fig. S7). This suggests that PATROL1 is required for efficient biomass production by localizing the proper amount of H^+-ATPase to the plasma membrane without downregulating its activity. Stomatal opening in response to environmental signals in *PATROL1*-overexpressing plants was rapid (Fig. 5, Supplementary Fig. S8), suggesting that PATROL1 may facilitate H^+-ATPase activation. Highly conserved PATROL1 orthologues appear commonly in higher plants (Fig. 1e, Supplementary Fig. S3). Taken together, our findings suggest that increases in biomass production in various plant species of interest may be achievable through manipulations of the function of *PATROL1* and related genes.

Methods

Plant material and growth conditions. All *Arabidopsis* lines used in this study, including a transgenic line expressing SLAC1–GFP[25], were derived from the Columbia (Col-0) background. EMS-mutagenized Col M_2 seeds were purchased from Lehle Seeds (Round Rock, TX, USA). Plants were grown on solid 1/2 MS medium for 18 days in a growth chamber (constant white light of 80 μmol m^{-2} s^{-1}

at 22 °C, 60% RH), and then transplanted into vermiculite pots supplemented with mineral nutrients. Under short-day condition, plants were grown on commercial soil (Supermix A, Sakata, Japan) in a growth chamber (8 h light of 127 μmol m^{-2} s^{-1} and 16 h dark at 23 °C, 60% RH).

Thermal imaging. Three-week-old plants were transferred to a growth cabinet (constant white light of 40 μmol m^{-2} s^{-1} at 22 °C, 43% RH) equipped with an automatic CO_2 control unit (FR-SP, Koito)[9]. Thermal images of plants were captured under different [CO_2] conditions using a thermography apparatus (TVS-8500, Nippon Avionics)[9].

Stomatal aperture response analysis. Three-week-old plants were incubated at the indicated [CO_2] in a growth cabinet. Abaxial epidermal peels of the plants were taken from the sixth or seventh leaf and were used immediately for aperture determination[9]. In FC treatment, epidermal peels were floated on a test medium containing 10 mM KCl, 10 mM Mes-KOH and 50 μM $CaCl_2$ (pH 6.15) and were incubated in the growth chamber. FC was added to the solution after 1 h of illumination and stomatal apertures were measured 2 h later[9]. The stomatal aperture was observed in epidermal peels with a digital camera attached to a microscope (BH2, Olympus, Tokyo Japan).

Stomatal conductance measurement. Gas exchange was measured on the aerial part of the 24-day-old seedlings using gas exchange systems (GFS3000, Heinz Walz, Effeltrich, Germany) equipped with a 3010-A *Arabidopsis* chamber[45]. The GFS3000 system was connected with a PC with data acquisition software (GFS-Win). The *Arabidopsis* cuvette was exposed to a light intensity of 200 μmol m^{-2} s^{-1} provided by a special artificial light (LED-Array/PAMFluorometer 3055-Fl, Heinz Walz, Effeltrich, Germany), with relative humidity and air temperature set to 50% and 22 °C, respectively. Measurements were made every minute.

Transgene construction. For functional complementation of the *patrol1* mutant, a fragment containing full-length *At5g06970* cDNA (accession number AY090450) was prepared from the RAFL 09-69-H21 clone, which was obtaind from RIKEN BioResource Center, Tsukuba, Japan, by digestion with *Not*I and *Bam*HI and subcloning into the vector pBluescript II KS^+. A *Sal*I-*Bam*HI fragment including the cDNA was cloned into the T-DNA vector pPZP2Ha3(−)[46]. For the production of 35S:*GFP–PATROL1*, the 35S promoter:*GFP* fragment with a glycine linker obtained by PCR using primers 5′-GGGCCCCTCGAGCCCCTCAGAAGA CCAGAGGGC-3′ and 5′-TACCGGTAGCACCTCCACCTCCCTTAT-3′ (the glycine linker site is underlined) with pKS(+)*GFP–OsGK1*[47] as a template, was inserted into pGEM-T Easy vector (Promega) to produce pG-35S:*GFP*. A DNA fragment containing the *PATROL1* ORF, obtained by PCR using primers 5′-GACC GGTATGGAAGAAGAAAATGCTGTC-3′ and 5′-GAGCTCCCCGGGGATCGT AAACTACAAACATTTGTA-3′, was inserted into the pGEM-T Easy vector to produce pG-*PATROL1*. The *Sac*II–*Age*I fragment of pG-35S:GFP1 containing the CaMV 35S promoter and *GFP* cDNA was inserted into the *Sac*II/*Age*I sites of pG-*PATROL1* to produce pG-35S:*GFP–PATROL1*. The *Xho*I-*Sma*I fragment of pG-35S:*GFP–PATROL1* was inserted into the *Xho*I/*Sma*I sites of pPZP2H-lac. For 35S:*GFP–AHA1*, a DNA fragment containing *AHA1* ORF was obtained by PCR using primers 5′-TATAAGGGAGGTGGAGGTGCTATGTCAGGTCTCGAAG-3′ and 5′-AGAACTAGTGGATCCCCCGGGTTTTAGAATTAAATTTAAATAT TAT-3′. The *Age*I/*Sma*I fragment obtained by digestion of the PCR-amplified *AHA1* was inserted together with an *Xho*I/*Age*I fragment of 35S:GFP into the *Xho*I/*Sma*I sites of pPZP2H-lac[46]. For 35S:RFP–AHA1 production, RFP was obtained by PCR using primers 5′-AGGATCCATGGCCTCCTCCGAGGA-3′ and 5′-CATAGC ACCTCCACCTCCCTTATA GGCGCCGGTGGAGTGGCGGC-3′ with mRFP plasmid as a template. A DNA fragment containing AHA1 ORF was obtained by PCR using primers 5′-GCCGCCACTCCACCGGCGCCTATAAGGGAGGTGGA GGTGCT-3′ and 5′-AGAACTAGTGGATCCCCCGGGTTTTAGAATTAAATTT AAATATTAT-3′. A DNA fragment containing RFP–AHA1 was obtained by PCR using primers 5′-AGGATCCATGGCCTCCTCCGAGGA-3′ and 5′-AGAACTAGT GGATCCCCCGGGTTTTAGAATTAAATTTAAATATTAT-3′ with RFP and AHA1 fragments as templates. The *Bam*HI/*Sma*I fragment obtained by digestion of the PCR-amplified RFP–AHA1 was inserted into *Bam*HI/*Sma*I sites of pPZP2Ha3. A *pPATROL1::GUS* construct was obtained by amplifying 2 kb of the *PATROL1* promoter region from genomic DNA using the oligonucleotides 5′-CGGTCGACA CAACCACTAGC-3′ and 5′-GGATCCCTCGATCCAGCTGCAATAAT-3′; the product was then inserted into the pGEM-T Easy Vector. A *Sal*I-*Bam*HI fragment including the *PATROL1* promoter sequences was cloned into the *Sal*I and *Bam*HI sites of pBI101.

Immunohistochemical analysis. Immunohistochemical detection of the plasma membrane H^+-ATPase in the epidermis was performed as described[33] with minor modifications. Plants were incubated under low CO_2 (<100 p.p.m.) for at least an hour. The abaxial epidermis of the rosette leaves was peeled with a forceps, and immediately incubated in 4% (*w*/*v*) formaldehyde in fixation buffer for 2.5 h at room temperature. The fixed epidermis was rinsed with water and attached to an MAS-coated glass slide. The samples were digested by cellulase solutions (1% Cellulase Onozuka R-10 (Yakult) and 0.1% Macerozyme R-10 (Yakult) in PBS) for 20 min at 37 °C. The samples were rinsed twice with PBS and permeabilized with 0.5% (*w*/*v*) Triton X-100 for 30 min, and then were blocked with 3% bovine serum albumin Fraction V. The samples were incubated with anti-plasma membrane H^+-ATPase (anti-AHA; Cosmo Bio) at a dilution of 1:1,000 for 16 h. The secondary antibody used here was Alexa Fluor 594 goat anti-rabbit IgG (Invitrogen; 1:500) for 3 h in the dark. After washing the samples, each specimen was mounted on a glass slide with 50% (v/v) glycerol.

Microscopy. The leaves were covered by a glass slide and observed under a fluorescence microscope (IX70, Olympus) equipped with an UPlanApo × 100/1.35 oil iris objective lens and a confocal scanning head (CSU10, Yokogawa). For staining endosomes, the seedlings were treated with 33 μM FM4-64 (Invitrogen), for 2 min and then washed with basal buffer (5 mM MES-Tris, 10 mM $CaCl_2$, 50 mM KCl, pH6.5). The hypocotyl epidermis was examined immediately. GFP and FM4-64 were excited with a laser (HPU-50101-PFS2; Furukawa) at 488 nm and the fluorescence was detected with a cooled CCD camera head system (CoolSNAP HQ, Photometrics) through a 524–546 nm band-pass filter (FF01-535/22-25, Semrock) for GFP, and a 604–644 band-pass filter (FF01-624/40-25, Semrock) for FM4-64. For light treatment, the leaves were irradiated with 200 μmol m^{-2} s^{-1} white light for 30 min with a cold light illumination system (LG-PS2, Olympus). In order to prevent drying, 3-mm-thick 1% agarose gels with basal buffer were placed onto the leaves[48]. For osmotic treatments, leaves were incubated in basal buffer (120 mOsM) or basal buffer with 0.4 M Mannitol (530 mOsM) for 15–30 min. Fluorescence from the secondary antibody, Alexa Fluor 594, was collected using a 561 nm laser (85-YCA-025-040, CVI Melles Griot) for excitation and a 580–600 nm band-pass filter (FF01-590/20-25, Semrock) for emission. For quantification of the Alexa Fluor 594 intensity, we measured the background-subtracted mean intensity in the signal regions that were segmented with Otsu's thresholding algorithm[49].

Isolation of guard cell and mesophyll cell protoplasts. GCPs from 600 to 1,200 leaves were isolated as described[25]. MCPs were isolated as described elsewhere[50] with some modifications. Twenty leaves from a 3–4-week-old plant were cut into 1-mm strips using a razor blade. Leaf strips were transferred into enzyme solution (5 mM MES (pH 5.6) containing 1% (*w*/*v*) cellulase R-10, 0.4% (*w*/*v*) macerozyme R-10, 0.1% (*w*/*v*) polyvinylpyrrolidone K-30 (PVP-40), 0.6 M mannitol, 0.5 mM $CaCl_2$, 0.5 mM $MgCl_2$ and 0.2% (*w*/*v*) BSA), and incubated at 24 °C for 2 h. Protoplasts were filtered through double layers of 50 μm nylon mesh and collected by centrifugation at 140 *g* for 4 min. GCP and MCP protoplasts were subjected to density gradient centrifugation at 200 *g* for 20 min using Histopaque-1077. The purity of the GCPs and MCPs were always higher than 97 and 99%, respectively.

Transgene expression analysis. Histochemical staining of GUS activity in *pPATROL1::GUS* transformants was assayed with 5-bromo-4-chloro-3-indolyl-D-glucuronide as a substrate[9]. To obtain tissue sections, GUS-stained samples were embedded in Technovit 8100 according to the manufacturers' instructions (Heraeus Kulzer GmbH, Wehrheim, Germany). A rotary microtome (Yamato Kohki) was used to cut 10-μm-thick sections. Total RNA from plant tissues or protoplasts were extracted and single-stranded cDNA synthesized from total RNA was used as RT-PCR templates according to the method described by Sugimoto *et al.*[51]. The RT-PCR primers for *PATROL1* were 5′-CTTCAGAGATATCGCCG GGA-3′ and 5′-CAATCCTGATGAGCTCTGAG-3′. An amplified 700-bp fragment of the *EF1α* cDNA was used as an internal standard[9]. Expression of *PATROL1* in guard cell and mesophyll cell protoplasts was examined by RT-PCR. The *HT1* gene was used as a guard-cell-specific expression control[9], and the *CBP* marker gene was used as a mesophyll-cell-specific expression control[52] using primers 5′-CTTATCTGGAGGTGCCACAA-3′ and 5′-CCTCACTCTTTCTTGGA TAAC-3′.

Water-loss measurement. The weight of detached rosette leaves was determined every 8 min. Three-week-old 1/2 MS plate-grown plants were used. Water loss was expressed as the percentage of initial fresh weight.

References

1. Willmer, C. M. & Fricker, M. D. *Stomata* 2nd edn (Chapman & Hall, London, 1996).
2. Hetherington, A. M. & Woodward, F. I. The role of stomata in sensing and driving environmental change. *Nature* **424,** 901–908 (2003).
3. Kim, T. H., Bohmer, M., Hu, H., Nishimura, N. & Schroeder, J. I. Guard cell signal transduction network: advances in understanding abscisic acid, CO_2, and Ca^{2+} signaling. *Annu. Rev. Plant Biol.* **61,** 561–591 (2010).
4. Schroeder, J. I., Raschke, K. & Neher, E. Voltage dependence of K^+ channels in guard-cell protoplasts. *Proc. Natl Acad. Sci. USA* **84,** 4108–4112 (1987).
5. Kinoshita, T. & Hayashi, Y. New insights into the regulation of stomatal opening by blue light and plasma membrane H^+-ATPase. *Int. Rev. Cell Mol. Biol.* **289,** 89–115 (2011).

6. Gaxiola, R. A., Palmgren, M. G. & Schumacher, K. Plant proton pumps. *FEBS Lett.* **581,** 2204–2214 (2007).
7. Merlot, S. *et al.* Constitutive activation of a plasma membrane H^+-ATPase prevents abscisic acid-mediated stomatal closure. *EMBO J.* **26,** 3216–3226 (2007).
8. Merlot, S. *et al.* Use of infrared thermal imaging to isolate *Arabidopsis* mutants defective in stomatal regulation. *Plant J.* **30,** 601–609 (2002).
9. Hashimoto, M. *et al. Arabidopsis* HT1 kinase controls stomatal movements in response to CO_2. *Nat. Cell Biol.* **8,** 391–397 (2006).
10. Richmond, J. E., Davis, W. S. & Jorgensen, E. M. UNC-13 is required for synaptic vesicle fusion in *C. elegans*. *Nat. Neurosci.* **2,** 959–964 (1999).
11. Augustin, I., Rosenmund, C., Südhof, T. C. & Brose, N. Munc13-1 is essential for fusion competence of glutamatergic synaptic vesicles. *Nature* **400,** 457–461 (1999).
12. Jahn, R. & Scheller, R. H. SNAREs--engines for membrane fusion. *Nat Rev.* **7,** 631–643 (2006).
13. Ma, C., Li, W., Xu, Y. & Rizo, J. Munc13 mediates the transition from the closed syntaxin-Munc18 complex to the SNARE complex. *Nat. Struct. Mol. Biol.* **18,** 542–549 (2011).
14. Basu, J. *et al.* A minimal domain responsible for Munc13 activity. *Nat. Struct. Mol. Biol.* **12,** 1017–1018 (2005).
15. Koch, H., Hofmann, K. & Brose, N. Definition of Munc13-homology-domains and characterization of a novel ubiquitously expressed Munc13 isoform. *Biochem. J.* **349,** 247–253 (2000).
16. Pei, J., Ma, C., Rizo, J. & Grishin, N. V. Remote homology between Munc13 MUN domain and vesicle tethering complexes. *J. Mol. Biol.* **391,** 509–517 (2009).
17. Li, W. *et al.* The crystal structure of a Munc13 C-terminal module exhibits a remarkable similarity to vesicle tethering factors. *Structure* **19,** 1443–1455 (2011).
18. Schmid, M. *et al.* A gene expression map of *Arabidopsis thaliana* development. *Nat. Genet.* **37,** 501–506 (2005).
19. Wang, Y. *et al.* Transcriptome analyses show changes in gene expression to accompany pollen germination and tube growth in *Arabidopsis*. *Plant Physiol.* **148,** 1201–1211 (2008).
20. Bolte, S. *et al.* FM-dyes as experimental probes for dissecting vesicle trafficking in living plant cells. *J. Microsc.* **214,** 159–173 (2004).
21. van Gisbergen, P. A., Esseling-Ozdoba, A. & Vos, J. W. Microinjecting FM4-64 validates it as a marker of the endocytic pathway in plants. *J. Microsc.* **231,** 284–290 (2008).
22. Kalla, S. *et al.* Molecular dynamics of a presynaptic active zone protein studied in Munc13-1-enhanced yellow fluorescent protein knock-in mutant mice. *J. Neurosci.* **26,** 13054–13066 (2006).
23. Ueno, K., Kinoshita, T., Inoue, S., Emi, T. & Shimazaki, K. Biochemical characterization of plasma membrane H^+-ATPase activation in guard cell protoplasts of *Arabidopsis thaliana* in response to blue light. *Plant. Cell Physiol.* **46,** 955–963 (2005).
24. Marmagne, A. *et al.* Identification of new intrinsic proteins in *Arabidopsis* plasma membrane proteome. *Mol. Cell. Proteomics* **3,** 675–691 (2004).
25. Negi, J. *et al.* CO_2 regulator SLAC1 and its homologues are essential for anion homeostasis in plant cells. *Nature* **452,** 483–486 (2008).
26. Vahisalu, T. *et al.* SLAC1 is required for plant guard cell S-type anion channel function in stomatal signalling. *Nature* **452,** 487–491 (2008).
27. Zhao, Z., Zhang, W., Stanley, B. A. & Assmann, S. M. Functional proteomics of *Arabidopsis thaliana* guard cells uncovers new stomatal signaling pathways. *Plant Cell* **20,** 3210–3226 (2008).
28. Cutler, S. R., Ehrhardt, D. W., Griffitts, J. S. & Somerville, C. R. Random GFP::cDNA fusions enable visualization of subcellular structures in cells of *Arabidopsis* at a high frequency. *Proc. Natl Acad. Sci USA* **97,** 3718–3723 (2000).
29. Hedrich, R. Ion channels in plants. *Physiol. Rev.* **92,** 1777–1811 (2012).
30. Eisenach, C., Chen, Z. H., Grefen, C. & Blatt, M. R. The trafficking protein SYP121 of Arabidopsis connects programmed stomatal closure and K^+ channel activity with vegetative growth. *Plant J.* **69,** 241–251 (2011).
31. Lisenbee, C. S., Karnik, S. K. & Trelease, R. N. Overexpression and mislocalization of a tail-anchored GFP redefines the identity of peroxisomal ER. *Traffic* **4,** 491–501 (2003).
32. Campbell, R. E. *et al.* A monomeric red fluorescent protein. *Proc. Natl Acad. Sci USA* **99,** 7877–7882 (2002).
33. Hayashi, M., Inoue, S., Takahashi, K. & Kinoshita, T. Immunohistochemical detection of blue light-induced phosphorylation of the plasma membrane H^+-ATPase in stomatal guard cells. *Plant Cell Physiol.* **52,** 1238–1248 (2011).
34. Turner, N. C. & Graniti, A. Fusicoccin: a fungal toxin that opens stomata. *Nature* **223,** 1070–1071 (1969).
35. Léon-Kloosterziel, K. M. *et al.* Isolation and characterization of abscisic acid-deficient *Arabidopsis* mutants at two new loci. *Plant J.* **10,** 655–661 (1996).
36. Südhof, T. C. The presynaptic active zone. *Neuron* **75,** 11–25 (2012).
37. Homann, U. & Thiel, G. Unitary exocytotic and endcytotic events in guard-cell protoplasts during osmotically driven volume changes. *FEBS Lett.* **460,** 495–499 (1999).
38. Shope, J. C., DeWald, D. B. & Mott, K. A. Changes in surface area of intact guard cells are correlated with membrane internalization. *Plant Physiol.* **133,** 1314–1321 (2003).
39. Grefen, C., Honsbein, A. & Blatt, M. R. Ion transport, membrane traffic and cellular volume control. *Curr. Opin. Plant Biol.* **14,** 332–339 (2011).
40. Besserer, A. *et al.* Selective regulation of Maize plasma membrane aquaporin trafficking and activity by the SNARE SYP121. *Plant Cell* **24,** 3463–3481 (2012).
41. Paciorek, T. *et al.* Auxin inhibits endocytosis and promotes its own efflux from cells. *Nature* **435,** 1251–1256 (2005).
42. Hager, A. Role of the plasma membrane H^+-ATPase in auxin-induced elongation growth: historical and new aspects. *J. Plant Res.* **116,** 483–505 (2003).
43. Gévaudant, F. *et al.* Expression of a constitutively activated plasma membrane H^+-ATPase alters plant development and increases salt tolerance. *Plant Physiol.* **144,** 1763–1776 (2007).
44. Haruta, M. *et al.* Molecular characterization of mutant *Arabidopsis* plants with reduced plasma membrane proton pump activity. *J. Biol. Chem.* **285,** 17918–17929 (2010).
45. Monda, K. *et al.* Environmental regulation of stomatal response in the *Arabidopsis* Cvi-0 ecotype. *Planta* **234,** 555–563 (2011).
46. Fuse, T., Sasaki, T. & Yano, M. Ti-plasmid vectors useful for functional analysis of rice genes. *Plant Biotechnol.* **18,** 219–222 (2001).
47. Sugimoto, H. *et al.* The rice nuclear gene, *VIRESCENT 2*, is essential for chloroplast development and encodes a novel type of guanylate kinase targeted to plastids and mitochondria. *Plant J.* **52,** 512–527 (2007).
48. Higaki, T. *et al.* Statistical organelle dissection of *Arabidopsis* guard cells using image database LIPS. *Sci. Rep.* **2,** 405 (2012).
49. Otsu, N. A threshold selection method from gray-level histograms. *IEEE Trans. Sys. Man. Cyber.* **9,** 62–66 (1979).
50. Yoo, S.-D., Cho, Y.-H. & Sheen, J. Arabidopsis mesophyll protoplasts: a versatile cell system for transient gene expression analysis. *Nat. Protoc.* **2,** 1565–1572 (2007).
51. Sugimoto, H. *et al.* The *virescent-2* mutation inhibits translation of plastid transcripts for the plastid genetic system at an early stage of chloroplast differentiation. *Plant Cell Physiol.* **45,** 985–996 (2004).
52. Mori, I. C. *et al.* CDPKs CPK6 and CPK3 function in ABA regulation of guard cell S-type anion- and Ca2 + -permeable channels and stomatal closure. *PLoS Biol.* **4,** e327 (2006).

Acknowledgements

We are grateful to N. Brose and L. Serna for critical reading of the manuscript, and E.M. Jorgensen, J.I. Schroeder and T. Teramoto for comments on the manuscript. We thank T. Sakaguchi for the technical assistance. We also thank R.Y. Tsien for making the mRFP gene available, and the Arabidopsis Biological Resource Center and Cereon Genomics for access to polymorphism information. This research was supported in part by Grants-in-Aid for 21114002 (K.I.), 24114007 (S.H.), 22114505 (S.H), 24228008 (K.S.), 25711017 (T.H.) and 24780046 (T.Y.) from the Ministry of Education, Science and Culture of Japan, and by the Program for Promotion of Basic and Applied Research for Innovations in Bio-Oriented Industry (K.I.), and the Advanced Measurement and Analysis grant from the Japan Science and Technology Agency (S.H.). M.H.-S. is grateful for the financial support from the Fumi Yamamura Memorial Foundation for Female Natural Scientists.

Author contributions

M.H.-S. and K.I. designed the studies and wrote the paper. M.H.-S. performed most of the experiments together with A.N., M.I., M.F., M.M., and J.N.; T.H., K.A. and S.H. performed imaging analysis with fluorescence microscope. T.Y. and K.S. measured fresh weight of the plants grown under short days. All authors discussed the results and commented on the manuscript.

Additional information

Supplementary Information accompanies this paper at http://www.nature.com/naturecommunications

Competing financial interests: The authors declare no competing financial interests.

Reprints and permission information is available online at http://npg.nature.com/reprintsandpermissions/

How to cite this article: Hashimoto-Sugimoto, M. *et al.* A Munc13-like protein in *Arabidopsis* mediates H^+-ATPase translocation that is essential for stomatal responses. *Nat. Commun.* 4:2215 doi: 10.1038/ncomms3215 (2013).